



The Aftershock Risk Index (ARI) – spatio-temporal quantification of aftershock impact after strong earthquakes

A.M. Schaefer⁽¹⁾, J.E. Daniell⁽²⁾, B. Khazai⁽³⁾, F. Wenzel⁽⁴⁾

⁽¹⁾ PhD Candidate (Dipl.-Ing., MSc.), Geophysical Institute & Center for Disaster Management and Risk Reduction Technology, Karlsruhe Institute of Technology, Germany, e-mail address: andreas.schaefer@kit.edu

⁽²⁾ Natural Hazards Risk Engineer & John Monash Scholar (Dr.-Ing.), Geophysical Institute & Center for Disaster Management and Risk Reduction Technology, Karlsruhe Institute of Technology, Germany, e-mail address: j.e.daniell@gmail.com

⁽³⁾ Researcher (PhD), Geophysical Institute, Karlsruhe Institute of Technology & Center for Disaster Management and Risk Reduction Technology, Karlsruhe Institute of Technology, Germany, e-mail address: bijan.khazai@gmail.com

⁽⁴⁾ Professor & Head of Geophysical Institute, Geophysical Institute & Center for Disaster Management and Risk Reduction Technology, Karlsruhe Institute of Technology, Germany, e-mail address: friedemann.wenzel@kit.edu

Abstract

The fear of aftershocks is one of the major psychological burdens of a society during the first days after strong earthquakes. In the aftermath, building stability is often unknown and the loss of human life due to the collapse of pre-damaged structures often makes recovery more difficult. Most recently, this effect was observed during the 2015 Gorkha earthquake sequence in Nepal in a few cases. There is an urgent need for a spatio-temporal aftershock risk indicator to provide affected stakeholders with appropriate measured information about the inherent risk.

Based on experience from various past events, aftershocks and triggered earthquakes have been observed as a significant contributor to socio-economic disaster impacts. A state-of-the-art aftershock activity metric for future earthquake events has been developed by assembling parameters of earthquake clustering based on global and regional studies of aftershock evolution. The activity metric is built from multiple non-linear optimisation procedures and machine learning methods and results in stochastic permutations of possible aftershock activity for the next day which are then translated into macroseismic intensity maps.

Since scientific maps with various indicators and statistical metrics are hard to transpose into daily life, an indicator system has been developed, which provides spatio-temporal scores for aftershock impacts. This study provides a first application example and indicates the need for a global implementation of such a system.

Keywords: Aftershock Prediction, Earthquake Risk, Disaster Communication

1. Introduction

Aftershocks are a well-known observation after strong earthquakes [1]. Frequent occurrence of aftershocks after a damaging mainshock induces a psychological burden [2] and often an intangible economic impact [3]. The expectation of upcoming strong aftershocks (often mixed with rumours [4]) often have a negative effect on recovery and disaster mitigation efforts. The estimates of an operationalized aftershock forecasting model in the context of an ongoing community-wide emergency can add new insights about aftershock risk to decision makers and general public, and would produce vital information, which, when combined with an effective awareness raising and risk communication program could alleviate a part of the stress and anxiety of populations struggling to recover in the direct aftermath of a major traumatic event. As discussed in the literature, the quality (specificity, consistency and certainty) and quantity (reinforcement) of aftershock risk warning information has a positive direct and indirect – through aftershock risk perception – effects on public warning response [5].

Following, the Mw 7.8 Nepal earthquake on April 25 which resulted in a high frequency of aftershocks we carried out a survey of 257 households in June 2016 on the fear of aftershocks among displaced populations to understand how this impacts their decisions to seek shelter [6]. It is important to note the frequency of aftershocks in the Nepal earthquake; by May 11 more than 60 aftershocks of magnitude 4 and larger were observed, several of them causing additional damage and fatalities. On May 12, a Mw 7.2 earthquake occurred further East on the Main Himalayan Thrust [7]. We found that across all affected areas, the fear of aftershocks was a key driver in the shelter behavior of displaced populations from damaged buildings. From the displaced population surveyed, 88% of those whose house was damaged but not destroyed indicated their house was still unsafe from aftershocks at the time of the interview (84% of those from urban areas and 93% of those from rural areas). 19.6% percent of all interviewed indicated safety from aftershocks as the primary reason for selecting their current shelter site, although this was more prevalent in urban areas. 75% of all interviewed indicated aftershocks as one of their main reasons for selecting their shelter. Our findings in Nepal agree with what is described in the literature ([8], [9], [10], [11]) as behaviour following a large earthquake when faced with aftershocks. Based on our survey results, an effective communication strategy of aftershock risk warning would have provided support to the decisions of displaced populations in seeking shelter after their building has been damaged.

There have been various approaches for aftershock prediction. The first approach for the quantification of aftershocks undertaken by [12] deriving the first temporal decay relationship, which was further advanced by [1] and known as the Omori-Utsu relationship. Today, various approaches consider the quantification of aftershocks in short time scales using self-consistent models, including the Early Aftershock Statistics (EAST) method of [13], the epidemic ETAS method (e.g. [14] or [15]), or short-term earthquake probability models (STEP) by [16]. This study introduces a new methodology to quantify and predict aftershock activity based on observations of previous aftershock sequences. It is based on the earthquake cluster analysis methodology of [17]. The assessment is hereby purely focused on aftershocks, which do not violate Bath's law [18], thus aftershocks which do not trigger their own distinct consecutive aftershock sequence. In the case of an aftershock prediction assessment of a new seismic sequence, it identifies earthquake clusters which are located close in space with a similar magnitude to the assessed main shock. It builds various aftershock decay functions using data fitting and parameter estimation methods and automatically identifies best fitting estimators based on a weighted logic optimisation. Since aftershock predictions have to be updated frequently in time, it utilises the modelling error to adjust the results for the next time step. Finally, intensity prediction maps are built based on stochastic modelling of possible aftershock activity for the next time window. Translating the intensity impact into a quantitative risk metric is difficult, since data on distinct aftershock damage is scarce and the financial impact of aftershocks is not significant (see section 3). Therefore the direct quantification of losses due to aftershocks was not included but instead are represented qualitatively using macro-seismic impact metrics in order to better represent the intangible nature of aftershock effects.

Tests are undertaken for a selection of 10 aftershock sequences in California, New Zealand, Italy, Greece and Nepal to provide a significantly wide range of possible case studies in different tectonic regimes and countries to prove its applicability for future assessments of aftershocks sequence predictions.

2. Aftershock Activity Forecasting

The total methodological frame of aftershock impact prediction consists of several steps, which are summarised briefly in this section. The steps comprise various methods of non-linear optimisation, machine learning and probabilistic seismic hazard assessments. The data foundation of each approach is an earthquake catalogue, comprising of as many events as possible, and which should be complete for all earthquakes at least $M_w > 4.0$ for the last 30 years to provide a sufficiently large data input. These catalogues have to be analysed by the Smart Cluster Method of [17] to have a sufficiently large number of pre-defined mainshock-aftershock sequences to build the data background of the aftershock decay fitting. The following process describes the methodology to predict the number of aftershocks and building aftershock impact maps within a predefined time window in the future, e.g. for the next 24 hours. The method is repeated consecutively in time, e.g. every 6h to build updated maps of future possible aftershock impacts. The method learns in each iteration from its own errors and adjusts its results based on most recent observations in comparison to previous modelling results. In case of a strong seismic event, e.g. with a minimum magnitude of $M_w = 6$, the method is initiated. This event is called the target event E_T . It is observed that the accuracy of the method increases with increasing mainshock magnitude.

2.1 Search for historic clusters similar in space and magnitude

Firstly, the provided database of earthquake clusters is searched for events which are similar in space and magnitude to E_T , hereby a nearest neighbour approach is applied [19], computing a uniform magnitude-space distance r , where a difference of $\Delta M_w = 1$ is equivalent to a distance of 250 km.

2.2 Determine aftershock decay parameters of these clusters

Each cluster considered as part of the E_T 's data neighbourhood is analysed for its aftershock statistics. Hereby, both an Omori-Utsu and a power-law approximation was applied and are shown in Eq. (1) and Eq. (2).

$$N(t) = K/(t+c)^p \quad (1)$$

$$N(t) = K e^{-\lambda t} \quad (2)$$

With N being the expected number of events at time t in days. The respective parameters of both functions are retrieved in several ways. The first way is via a weighted mean of the 10 closest clusters found in step 1, where the weighting is considered inversely to distance $1/r$. For each cluster the formulas are resolved in a cumulative and a non-cumulative way, leading to slightly different parameter results. In addition, while c , p and λ are shaping parameter of the decay, K represents in both equations the overall productivity of the sequence. Instead of inferring K from the nearest clusters, K can be directly estimated using non-linear least squares fitting of the provided functions and shaping parameters on the so-far observed events in E_T , which is only considered for the cumulative case. A third way to retrieve aftershock decay statistics is to directly fit both equations on the so-far observed events, however this approach is difficult and needs enough data to capture the decay curvature. This leads to a total of 8 statistical approximations of aftershock decay for the current sequence.

2.3 Adjust aftershock decay functions based on so-far observed events

From the resulting 8 representations of aftershock decay, a weighted superposition is computed to find the best mix of decay functions to approximate the so-far observed decay. In some cases, these representations cannot capture the observed activity well enough, thus 2 more approximations are built by fitting a weighted superposition to both by a factor of 2 of the increased or decreased aftershock activity. In case the model is consecutively under- or over predicting, it utilises this deviation for the next iteration by directly increasing or decreasing the model result considering the 2 above mentioned increased and decreased fits.

2.4 Estimate mean number of events for next time window

After each iteration the number of expected aftershocks is computed. In addition, the error in term of $|N_M - N_O|/N_O$ is computed for all previous time steps and used as the major quality metric. Hereby N_M is the number of modelled events for the next time step and N_O is the number observed events. The algorithm stores

consecutively the error and its respective trend. When estimating the mean expected number of aftershocks for the next time window, it adjusts this number by the observed error trend. In case the algorithm keeps underpredicting by 10%, it increases the expected number by 10%, if the error was oscillating between over- and underprediction, it will most likely not change the expected number since no trend is visible in such a case.

2.5 Model stochastic versions of possible aftershock sequences in next time window

To build a sufficiently wide range of possible aftershock sequences within the next time window, a large number of permutations are modelled stochastically. The number of expected events follows a normal distribution using the mean number of expected events previously computed and a standard deviation which is twice the quotient of error to the mean of the iteration before. In this study, 2500 permutations are considered appropriate. The minimum magnitude is either the minimum magnitude of the provided earthquake catalogue or at least $M_w=3$. To compute an appropriate magnitude distribution of the stochastic aftershock sequences, the weighted mean of Gutenberg-Richter b-values of the nearest clusters of step 1 is computed. In the case that at least 200 events have been observed so-far, the b-value of the current cluster is computed as well while neglecting the mainshock. The so-far observed aftershocks also provide the information for the normal distribution of earthquake depths. The location of each event is linked probabilistically to a smooth seismicity representation of the so-far observed events similar to the method of [20].

2.6 Test of earthquake forecast

As an internal sanity check, the derived stochastic catalogues are tested on a log-likelihood scale similar to other earthquake prediction algorithms (e.g. [21]). The proposed log-likelihood tests used in the CSEP framework, summarized by [22]. In this study, the L-, S-, M- and N- tests are used to check the probabilistic reliability of the forecast. They test the general likelihood, spatial likelihood, magnitude likelihood and number likelihood of the observation matching the proposed forecast probabilities.

2.7 Compute intensity probability distribution for locations of interest

With a large number of possible aftershock sequence permutations, a probability range of the possible aftershock impact within the next time window can be built. The region around the main shock is gridded regularly on a resolution of 1 km. For each grid point, the intensity of each possible permutation is calculated. Only pixels where at least once an intensity of $MMI \geq 3$ was observed are considered. The intensity is calculated using published macroseismic intensity prediction equations appropriate for the location where the aftershock sequence occurs. For each pixel, the probability of all permutations to observe a certain intensity is calculated.

2.8 Translate intensity probability distribution into simple aftershock impact metric

Since the macroseismic intensity is still an engineering metric, a simpler and easier to communicate metric has to be introduced. Intensities are simplified into 4 classes, by simply considering intensities larger than 6 as “damaging (red)”, intensities between 4.5 and 6 as “heavily felt/slightly damaging (orange)”, intensities 3 to 4.5 as “felt (yellow)” and any intensity below 3 as “not felt (green)/felt slightly”, thus ending up with a probability for 4 classes, which are provided for each pixel surrounding the on-going seismic sequence.

The last step introduces a simplification of earthquake impact metrics to make them easier to communicate into a non-scientific community. The 4 classes are considered the most simplistic ways to experience an earthquake where, a person can either feel or not feel it. While feeling it, it should be considered 2 classes of shaking, slight and heavy. The final stage to be simply called as damaging is related to the large amount of uncertainties constrained to aftershock impacts, pre-damaged structures may be closer to collapse and empirical data is only scarcely available thus a more diverse metric is unrealistic to put in place and not reliable enough for public communication. This follows the damage scale closely of [23]. Since 4 probabilities are difficult to put into a single map, a conservative mesh-up of these results is put into place, thus a traffic-light approach was considered where; green: $P > 70\%$ not feel an aftershock, yellow: $P > 10\%$ to experience shaking, if additionally the probability of experiencing heavy shaking is $P > 10\%$, then its orange and if even a further probability of a damaging event is larger than 2%, the pixel is red. This metric is still under review and provides a preliminary model. This methodology is still under development and will be subsequently improved in future editions.

3. Socio-Economic Aftershock Impact

Aftershock risk is inherently difficult to quantify given the pre-damaged state of most buildings after a large earthquake. Although the premise may be that an aftershock will deliver greater damage ratios than the original shock; often this is only observed in major sequential earthquakes and larger aftershocks (ca. M0.5 less than aftershock with the desirable exposure). Many authors have examined the vulnerability and fragility functions of aftershocks with [24] examined incremental damage as a result of aftershocks, assuming a continuation of the cyclic response, considering the ductility capacity to collapse as the structural damage measure enabling approximate-form solutions for reliability following on from [25]. In [26] in the wake of the Christchurch sequence, show the damage-interaction with an increasing fragility by exploring damage states from an initial main shock and the resultant aftershock. [27] shows that aftershocks typically affect structures within a small magnitude difference, and short aftershock distance, but do not affect structures in most sequences. Due to the definition of aftershock in the case of this aftershock risk index, traditional damaging sequences such as Christchurch had a much more limited effect given the treatment of the February 2011 earthquake as a new earthquake. Using [28], the socioeconomic effects of aftershock sequences have been reviewed.

Table 1 – Overview of socio-economic loss contribution from aftershocks for all 17 test cases with respective date and magnitude. The latitude and longitude coordinates reflect the centroid of the aftershock sequence.

| Sequence | Economic Damage (as % of mainshock) | Fatalities (as % of mainshock) | Disruption to rescue/recovery |
|----------------------|----------------------------------------|-----------------------------------|-------------------------------|
| Darfield, NZ | <1% | 0 | In first 7 hrs |
| Christchurch, NZ | 1-3 % | 0 | Years of disruption |
| L'Aquila, Italy | <1% | 0 | Yes, ca. 7 days |
| Denali, USA | 0 | 0 | No |
| Baja California, USA | <0.1% | 0 | No |
| Northridge, USA | ca. 0.1% | 0 | Yes, ca. 2 weeks |
| Loma Prieta, USA | <0.1% | 0 | Yes, ca. 2 weeks |
| Landers, USA | <0.1% | 0 | No |
| Gorkha, Nepal (7.8) | <1% | 15 deaths (ca. 0.17%) | Yes, ca. 3 weeks |
| Dolakha, Nepal (7.2) | <1% | 6 deaths (ca. 4%) | Yes, 1 week |

In the Christchurch Sequence, [29] describes 17 events in the sequence with insurance effects and [30] shows the effect of all earthquakes from 2010 to 2012 outside of the main 3 earthquakes in Sep 2010, Feb 2011 and June 2011. Around 5% of losses resulted from these additional earthquakes, however a significant proportion from the December 2011 earthquake, therefore totalling around 2%. The intangible interruption to life and the disruption to rescue efforts likely caused a greater amount of socioeconomic loss than the actual damage from aftershocks. The immediate aftershocks in the first few hours, caused damage, however, this damage was not great compared to the mainshock (however hampered rescue efforts in the few days after the mainshock).

In a number of USA earthquakes studied, there was very low damage from aftershocks: a) 2010 Baja California quake, there were bottles off shelves in resulting aftershocks; b) 1994 Northridge, there was only a bit of infrastructure damage from the 20 March 1994 quake; c) 1989 Loma Prieta, there was minor damage, 1 collapse, minor power failures. Other quakes studied had minimal effects. In the Nepal earthquake, the large triggered quake of 12th May 2015, caused an additional 2.5% of deaths (ca. 230 compared to 9050+ in the mainshock). Both earthquakes had local aftershocks which caused a number of deaths. The Gorkha earthquake had ca. 15 deaths from 5 aftershocks. The Sindhupalchok M7.2 had ca. 6 deaths from 3 aftershocks. The economic damage associated with the Sindhupalchok earthquake was in the order of 3% of the original earthquake.

The definition of aftershocks within insurance contracts was a key aspect of the 2011 Christchurch earthquake and other events. In reinsurance CAT XL contracts or insurance contracts, 72 or fixed hour clauses are often employed, with any aftershock within this time being defined as part of the mainshock.

“It is agreed that any loss of or damage to the insured property arising during any one period of 72 consecutive hours, caused by storm, cyclone, tempest, flood or earthquake shall be deemed as a single event and therefore to constitute one occurrence with regard to the Deductibles stated in the Schedule. For the purpose of the foregoing the commencement of any such 72 hour period shall be decided at the discretion of the Insured, it being understood and agreed, however, that there shall be no overlapping in any one, two or more such 72 hour periods in the event of loss or damage occurring over a more extended period of time.”

An issue in multiple events is often that the insured is entitled to multiple payments in certain insurance clauses. i.e. if the first earthquake causes partial damage to a structure; and then the second earthquake a few months later completely damages the structure beyond repair. A good example of this was the Ridgecrest NZ Limited v IAG New Zealand Limited case where a commercial building in the September and December 2010 earthquakes was damaged and during this time repairs were started. The building was then damaged beyond repair later in the 2011 February, June and December earthquakes in Christchurch. If repairs had not been started it would be likely that only the total cost would have to have been paid out. There were many other cases that also ended up in the courts based on the issue of sequential losses. The combination of various clauses globally relating to aftershock and sequential damage definitions make the risk index a useful tool; but often such decisions to payouts are often based on assessing the potential losses associated with each aftershock or “new event”, and attempting to deconstruct what damage occurred in each event via surveys or photographic evidence (see [31] and [32], see Table 2).

Table 2 – Overview of earthquake loss contributions from the 2010-2011 Darfield-Christchurch sequence, adopted from [31].

| Date of Earthquake | Repair Cost | | | Totals |
|--------------------|--------------|----------------|----------------|----------------|
| | Contribution | Per Event | GST | |
| 4.9.2010 | 22 % | \$2,641,716.38 | \$396,257.46 | \$3,037,973.83 |
| 26.12.2010 | 1 % | \$120,078.02 | \$18,011.70 | \$138,089.72 |
| 22.02.2011 | 61 % | \$7,324,759.04 | \$1,098,713.86 | \$8,423,472.90 |
| 16.4.2011 | 2 % | \$240,156.03 | \$36,023.41 | \$276,179.44 |
| 13.6.2011 | 14 % | \$1,681,092.24 | \$252,163.84 | \$1,933,256.08 |

Table 3 – Overview of all 10 test cases with respective date and magnitude. The latitude and longitude coordinates reflect the centroid of the aftershock sequence.

| Event-Name | Date (LT) | Mw | Location (Lat/Long) | Country / State | I ₀ | M4 (48h) |
|----------------------|------------|-----|---------------------|-----------------|----------------|----------|
| Loma Prieta 1989 | 1989-10-17 | 6.6 | 33.01°N, 115.82°W | California | IX | 9 |
| Landers 1992 | 1992-06-28 | 7.3 | 34.33°N, 116.47°W | California | IX | 51 |
| Northridge 1994 | 1994-01-17 | 6.7 | 34.30°N, 118.54°W | California | IX | 30 |
| Kozani 1995 | 1995-05-13 | 6.6 | 40.13°N, 21.68°E | Greece | IX | 44 |
| Denali 2002 | 2002-11-03 | 7.9 | 63.34°N, 146.28°W | Alaska | IX | 69 |
| L'Aquila 2009 | 2009-04-06 | 6.3 | 42.36°N, 13.42°E | Italy | VIII | 16 |
| Baja California 2010 | 2010-04-04 | 7.2 | 32.42°N, 115.51°W | California | IX | 53 |
| Darfield 2010 | 2010-09-04 | 7.1 | 43.55°S, 172.24°E | New Zealand | IX | 204 |
| Christchurch 2011 | 2011-02-21 | 6.3 | 43.57°S, 172.75°E | New Zealand | IX | 93 |
| Gorkha 2015 | 2015-04-25 | 7.8 | 28.15°N, 84.71°E | Nepal | IX | 140 |

Table 4 – Overview of likelihood test results for 10 case study aftershock sequences. Bold numbers indicate that the forecast is inconsistent with the observation for the respective likelihood test.

| Event | | 1 Day | 2 Days | 3 Days | 4 Days | 5 Days | 7 Days | 10 Days |
|----------------------|--------------|--------------|--------------|--------------|--------------|--------------|--------------|--------------|
| Loma Prieta 1989 | L γ | 1.000 | 0.975 | 0.851 | 0.719 | 0.951 | 0.532 | 0.989 |
| | N δ_1 | 0.305 | 0.504 | 0.494 | 0.265 | 0.585 | 0.680 | 0.282 |
| | N δ_2 | 0.695 | 0.496 | 0.506 | 0.735 | 0.415 | 0.320 | 0.718 |
| | M κ | 0.969 | 0.805 | 0.777 | 0.976 | 0.980 | 0.124 | 0.998 |
| | S ζ | 0.923 | 0.797 | 0.207 | 0.815 | 0.689 | 0.693 | 0.290 |
| Landers 1992 | L γ | 1.000 | 1.000 | 1.000 | 0.990 | 0.124 | 0.004 | 0.993 |
| | N δ_1 | 0.798 | 0.792 | 0.356 | 0.465 | 0.581 | 0.878 | 0.758 |
| | N δ_2 | 0.202 | 0.208 | 0.644 | 0.535 | 0.419 | 0.122 | 0.242 |
| | M κ | 0.999 | 1.000 | 1.000 | 1.000 | 0.721 | 0.004 | 1.000 |
| | S ζ | 0.948 | 0.948 | 0.618 | 0.108 | 0.490 | 0.858 | 0.153 |
| Northridge 1994 | L γ | 0.988 | 0.916 | 0.999 | 0.595 | 0.904 | 0.450 | 0.119 |
| | N δ_1 | 0.340 | 0.541 | 0.328 | 0.538 | 0.539 | 0.268 | 0.656 |
| | N δ_2 | 0.660 | 0.459 | 0.672 | 0.462 | 0.461 | 0.732 | 0.344 |
| | M κ | 0.998 | 0.649 | 1.000 | 0.421 | 0.637 | 0.888 | 0.230 |
| | S ζ | 1.000 | 0.014 | 0.996 | 0.987 | 0.001 | 0.958 | 0.814 |
| Kozani 1995 | L γ | 0.014 | 0.550 | 0.102 | 0.047 | 0.469 | 0.173 | 0.010 |
| | N δ_1 | 0.382 | 0.496 | 0.485 | 0.678 | 0.700 | 0.823 | 0.662 |
| | N δ_2 | 0.618 | 0.504 | 0.515 | 0.322 | 0.300 | 0.177 | 0.338 |
| | M κ | 0.019 | 0.361 | 0.032 | 0.094 | 0.389 | 0.275 | 0.248 |
| | S ζ | 0.988 | 0.179 | 0.616 | 0.120 | 0.389 | 0.637 | 0.308 |
| Denali 2002 | L γ | 0.880 | 1.000 | 0.770 | 0.000 | 0.603 | 0.093 | 0.545 |
| | N δ_1 | 0.310 | 0.546 | 0.348 | 0.994 | 0.850 | 0.700 | 0.459 |
| | N δ_2 | 0.690 | 0.454 | 0.652 | 0.006 | 0.150 | 0.300 | 0.541 |
| | M κ | 0.988 | 0.999 | 0.933 | 0.009 | 0.681 | 0.095 | 0.784 |
| | S ζ | 0.270 | 0.521 | 0.280 | 0.000 | 0.542 | 0.024 | 0.010 |
| L'Aquila 2009 | L γ | 1.000 | 0.998 | 1.000 | 1.000 | 0.978 | 0.780 | 0.703 |
| | N δ_1 | 0.403 | 0.633 | 0.561 | 0.334 | 0.613 | 0.897 | 0.442 |
| | N δ_2 | 0.597 | 0.367 | 0.439 | 0.666 | 0.387 | 0.103 | 0.558 |
| | M κ | 0.890 | 0.962 | 1.000 | 1.000 | 0.993 | 0.562 | 0.777 |
| | S ζ | 1.000 | 0.991 | 0.000 | 0.606 | 0.976 | 0.140 | 0.001 |
| Baja California 2010 | L γ | 0.917 | 0.798 | 0.031 | 0.227 | 0.096 | 0.160 | 0.008 |
| | N δ_1 | 0.776 | 0.607 | 0.366 | 0.351 | 0.672 | 0.190 | 0.643 |
| | N δ_2 | 0.224 | 0.393 | 0.634 | 0.649 | 0.328 | 0.810 | 0.357 |
| | M κ | 1.000 | 0.986 | 0.435 | 0.620 | 0.441 | 0.703 | 0.037 |
| | S ζ | 0.967 | 0.312 | 0.166 | 0.715 | 0.764 | 0.076 | 0.997 |
| Darfield 2010 | L γ | 0.000 |
| | N δ_1 | 0.750 | 0.509 | 0.341 | 0.422 | 0.770 | 0.138 | 0.220 |
| | N δ_2 | 0.250 | 0.491 | 0.659 | 0.578 | 0.230 | 0.862 | 0.780 |
| | M κ | 0.952 | 0.330 | 0.000 | 0.000 | 0.005 | 0.000 | 0.000 |
| | S ζ | 0.832 | 0.898 | 0.229 | 0.996 | 0.663 | 0.920 | 0.893 |
| Christchurch 2011 | L γ | 0.000 |
| | N δ_1 | 0.567 | 0.228 | 0.482 | 0.552 | 0.364 | 0.463 | 0.170 |
| | N δ_2 | 0.433 | 0.772 | 0.518 | 0.448 | 0.636 | 0.537 | 0.830 |
| | M κ | 0.855 | 0.752 | 0.009 | 0.110 | 0.000 | 0.072 | 0.048 |
| | S ζ | 0.994 | 0.558 | 0.828 | 0.998 | 0.939 | 0.998 | 0.001 |
| Gorkha 2015 | L γ | 0.202 | 0.193 | 0.316 | 0.248 | 0.628 | 0.096 | 0.526 |
| | N δ_1 | 0.871 | 0.855 | 0.314 | 0.991 | 0.489 | 0.568 | 0.369 |
| | N δ_2 | 0.129 | 0.145 | 0.686 | 0.009 | 0.511 | 0.432 | 0.631 |
| | M κ | 0.174 | 0.181 | 0.711 | 0.326 | 0.702 | 0.428 | 0.923 |
| | S ζ | 0.874 | 0.884 | 0.072 | 0.224 | 0.257 | 0.120 | 0.984 |

4. Case Study

For this study, the methodology was tested on various strong seismic sequences all around the world. 7 countries and states have been assessed considering 10 different event sequences since 1989 in California, Alaska [33], New Zealand (see acknowledgement), Italy [34] and Greece [35]. While for all these regions, moderate to high quality seismic catalogues are available, the method was also assessed for regions with a significantly worse data quality, hereby the 2015 Nepal earthquake was considered as a test case, where the magnitude of completeness is about $M_c=4.0$. The Emilia Romagna earthquake of 2012 in Italy is slightly below the method magnitude threshold of 6.0 and thus considered a test case for this threshold magnitude. All catalogues were set to a minimum magnitude of M_w 2.5. Each sequence was modelled subsequently for the first 1 to 14 days of aftershock activity. While for the majority, most sequences last longer, the most significant amount of aftershock events occur normally within the first two weeks and especially for sequences with only moderately strong main shocks, e.g. in Italy, the aftershocks reduce significantly in strength within days after the main shock. Table 3 provides an overview of the event selection of this study.

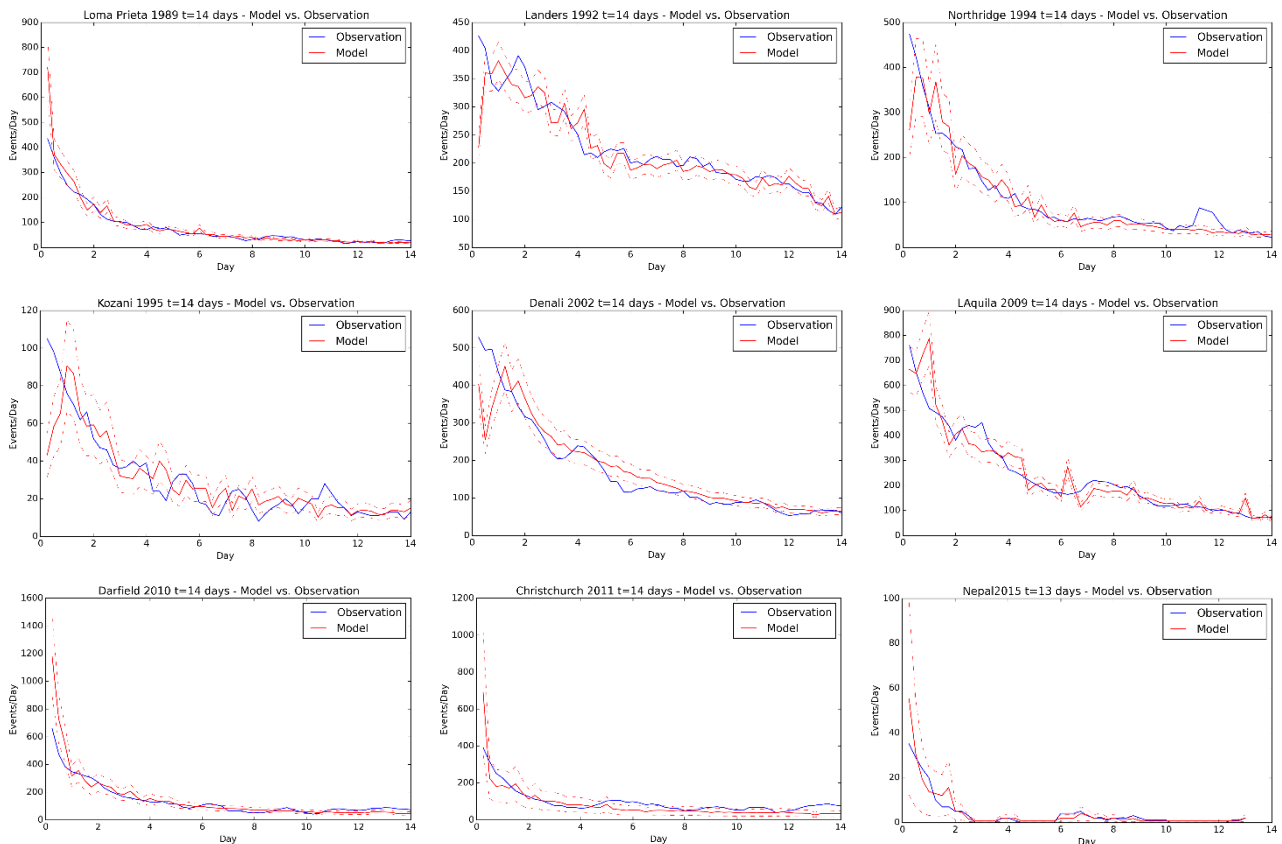


Fig. 1 – Comparison of the 9 aftershock sequences, the 2010 Baja California sequences is shown in Fig. 2. Each diagram compares the observed number of aftershocks (blue) for each for the next 24h at each time step with the modeled mean number and its respective standard deviation (red). The shown model result is hereby not corrected for consecutive errors.

An important element of aftershock sequence prediction is to appropriately define what an aftershock actually is. In this study and the whole methodology, aftershocks are earthquakes which occur close in space and time after a strong seismic event ($M_w > 6.0$). In case a very strong aftershock occurs, which normally has a magnitude difference of $\Delta M_w < 1.0$ and which is located along the perimeter of the so-far observed aftershocks, it is most likely considered a subsequent rupture, as observed in California, when the 1992 Landers earthquake triggered within hours the Joshua Tree earthquake located on another fault. Similarly in 2015 in Nepal, where about 2 weeks after the M_w 7.8 main shock, a M_w 7.2 event continued the rupture further to the east, or in New Zealand, where the rupture of the 2010 Darfield earthquake continued 2011 in Christchurch. All these so-called

“subsequent rupture events” are not considered an aftershock as part of this study. These events trigger their own distinct aftershock sequences, thus the whole process can no longer be quantified by one of the above introduced equations, like the Omori-Utsu equation and are thus not predictable by the proposed methodology. The event selection was limited to strong seismic and well-studied events, preferably with a significant intensity impact. For each location, a brief selection of macro seismic intensity prediction equations was introduced to build the intensity impact maps. This selection is a crucial element of the whole methodology and should be treated carefully; hereby it is important to consider the aftershock impact on pre-damaged structures and the fact that most of the aftershock events only have moderate magnitudes. For California [36] was chosen, for New Zealand [37], for Nepal [38], for Greece [39] and for Italy [37] and [40]. For Italy, the 50% weighted average of the two selected intensity functions was used. Table 4 shows the results of the likelihood tests for 7 different times of assessment (1, 2, 3, 4, 5, 7 and 10 days). The forecasts are tested using the likelihood tests of [22] (see section 2.6). Hereby, a forecast is considered consistent with the observation if the quantile score is larger than a threshold $\alpha=0.05$ for quantiles γ , ζ and κ and $\alpha=0.025$ for δ_1 and δ_2 [41]. Inconsistent forecasts are shown in bold. It can be seen that a majority of test results is within the accepted quantile and thus the forecasts are considered consistent with the observation of aftershocks of the selected time window. In total, about 12.5 % of all tests failed and where inconsistent. 50% of these failures are associated with the L-test indicating the combined likelihood of magnitude and location was insufficiently predicted. Thus could indicate that the occurrence of strong aftershocks is not correlated with the general event density of smaller aftershocks.

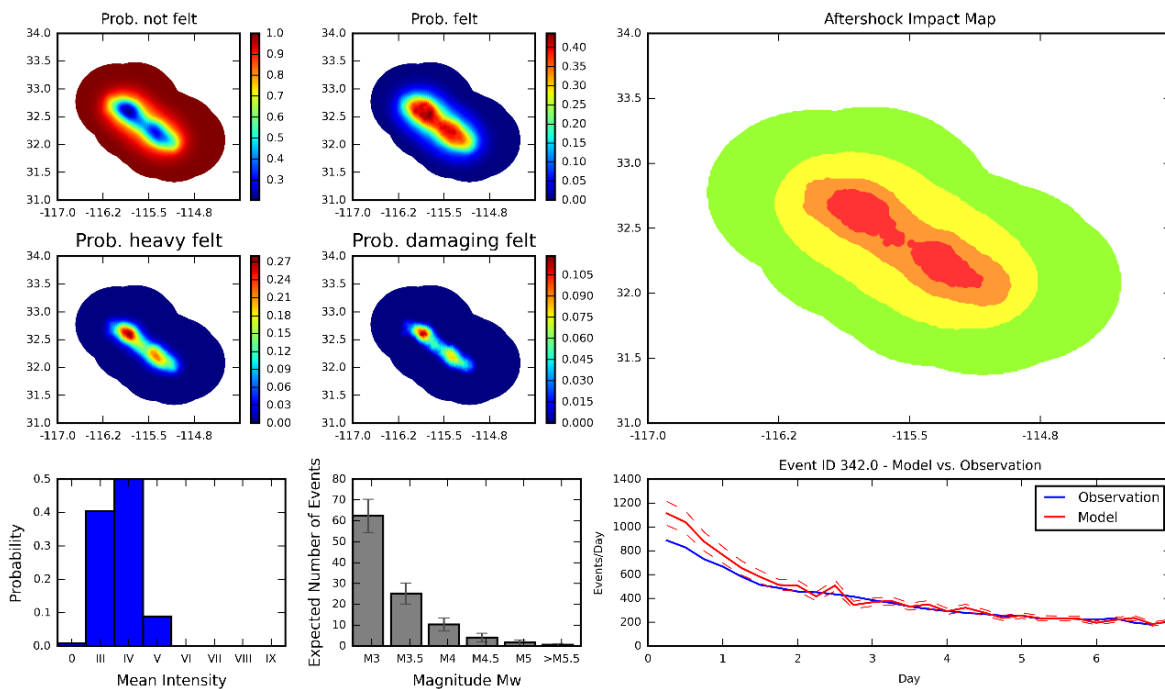


Fig. 2 – Selection of aftershock impact metrics for the 7th day after the 2010 Baja California earthquake: Top left show the probability maps of the 4 impact classes. Top right: General aftershock impact map. For both, x- and y-axis are longitude and latitude respectively. Bottom right: the mean expected aftershock rate of the model compared to the actual observed activity. Bottom left: probability range of mean aftershock intensities and bar chart for the expected number of earthquakes per magnitude within the next 24h.

5. Discussion & Conclusion

This study introduced a new and reliable methodology to predict aftershock activity for certain time-windows in near real-time during on-going strong seismic sequences. It has been observed, especially most recently in the 2015 Nepal earthquake, but also many times before in the past, that aftershocks induce a major psychological burden on the affected society and additionally makes immediate recovery more difficult [3]. The

goal of this study was to introduce a method, which provides metrics on the average expectancy of direct aftershock impacts on a short time scale, e.g. for the next 24h, but is limited to moderate aftershocks which do not violate the Båth's law [18] and which do not trigger their own dominant aftershock sequence. It uses various non-linear optimisation methods and utilises machine learning processes to retrieve these estimates. It was tested on 12 different aftershock sequences in 5 countries to test its reliability. Except for minor scattering which can be expected for complex and chaotic processes like aftershock occurrence, the results show a reasonable consistency with the retrospectively observed values. This was additionally underlined by 85% success rate of 4 different likelihood tests. The general activity forecast was then translated using macroseismic intensity prediction equations into a communicable impact scale. Considering 4 classes of possible impacts is highly valuable to people and organizations in the regions giving the probabilities of not feeling an aftershock, just feeling it, heavily feeling it with expecting minor damage and to expect major damage. This fulfils the most fundamental information demands in such events. With respect to a historic study which was also undertaken, the necessity of calculating direct loss impacts is not given, thus in terms of socio-economic numbers, aftershocks as defined in this paper only have an insignificant contribution to losses.

A traffic light system provides a useful tool for decision makers and the public to understand. GDACS employs a 3 tier system with green indicating a Moderate event, International Assistance not likely; orange with local disaster where International Assistance might be required and red indicating a severe disaster with International Assistance is expected to be required. USGS-PAGER employs such a traffic light system (albeit Red, Orange, Yellow and Green) for event alerts over a logarithm scale to show the relative impact. This system follows both schemes by employing red and orange as the damaging scales, with green and yellow indicating little damage providing an easy to understand view for users.

For future developments, the currently visible oscillation of the aftershock expectation metric will be analysed further to stabilise the results in general together with an increase of accuracy for the first 48h. In addition, a detailed probability assessment about the occurrence of the strongest aftershock is recommended and testing the actual aftershock magnitude distribution of the stochastic model against the past observations.

7. Acknowledgements

We acknowledge the New Zealand GeoNet project and its sponsors EQC, GNS Science and LINZ, for providing data/images used in this study. Furthermore, we thank the anonymous reviewer of this manuscript for the helpful comments.

8. References

- [1] T. Utsu, "Magnitude of earthquakes and occurrence of their aftershocks," *Journal of Seismology of Japan*, vol. 10, pp. 35-45, 1957.
- [2] R. Rancone, L. Giusti, M. Mazza, V. Bianchini, D. Ussorio, R. Pollice and M. Casacchia, "Persistent fear of aftershocks, impairment of working memory, and acute stress disorder predict post-traumatic stress disorder: 6-month follow-up of help seekers following the L'Aquila earthquake," *SpringerPlus*, vol. 2, no. 636, 2013.
- [3] M. Dorahy, C. Ranouf, A. Rowlands, D. Hanna, E. Britt and J. Carter, "Earthquake Aftershock Anxiety: An Examination of Psychosocial Contributing Factors and Symptomatic Outcomes," *Journal of Loss and Trauma: International Perspectives on Stress & Coping*, vol. 21, no. 3, pp. 246-258, 2016.
- [4] T. Y., Y. Sakamoto and T. Matsuka, "Transmission of Rumor and Criticism in Twitter after the Great Japan Earthquake," in *34th Annual Meeting of the Cognitive Science Society*, Sapporo, Japan, 2012.
- [5] D. Mileti and P. O'Brien, "Warnings during disaster: Normalizing communicated risk," *Social Problems*, pp. 40-57, 1992.
- [6] B. Khazai, T. Girard, J. Anhorn, S. Brink, G. Kumar, B. Parajuli, S. Wagle and O. Khanal, "Emergent issues and

- vulnerability factors in temporary and intermediate shelters following the 2015 Nepal earthquake,” *International Journal of Mass Emergencies and Disasters*, vol. in review.
- [7] L. Adhikari, U. Gautam, B. Koirala, M. Bhattarai, T. Kandel, R. Gupta, C. Timsina, N. Maharjan, T. Dahal, R. Hoste-Colomer, Y. Cano, M. Dandine, A. Guilhem, S. Merrer, P. Roudil and L. Bollinger, “The aftershock sequence of the 2015 April 25 Gorkha-Nepal earthquake,” *Geophys. J. Int.*, vol. 203, pp. 2119-2124, 2015.
- [8] C. Hsu, M. Chong, P. Yang and C. Yen, “Posttraumatic stress disorder among adolescent earthquake victims in Taiwan,” *Journal of the American Academy of Child & Adolescent Psychiatry*, vol. 41, no. 7, pp. 875-881, 2002.
- [9] H. Kuwabara, T. Shiori, S. Toyabe, T. Kawamura, M. Koizumi, M. Ito-Sawamura and T. Someya, “Factors impacting on psychological distress and recovery after the 2004 Niigata-Chuetsu earthquake, Japan,” *Psychiatry and Clinical Neuroscience*, vol. 62, no. 5, pp. 503-507, 2008.
- [10] J. Hall, W. Holmes and S. P, “Northridge earthquake,” Preliminary reconnaissance report, January 17, 1994.
- [11] M. Erdik, Y. Kamer, M. Demircioğlu and K. Şeşetyan, “23 October 2011 Van (Turkey) earthquake,” *Natural Hazards*, vol. 64, no. 1, pp. 651-665, 2012.
- [12] F. Omori, “On the aftershocks of earthquakes,” *Journal of the College of Science, Imperial University of Tokyo*, vol. 7, pp. 111-200, 1894.
- [13] P. Shebalin, C. Narteau, M. Holschneider and D. Schorlemmer, “Short-Term Earthquake Forecasting Using Early Aftershock Statistics,” *Bulletin of the Seismological Society of America*, vol. 101, no. 1, pp. 297-312, 2011.
- [14] Y. Ogata, “Statistical Models for Earthquake Occurrences and Residual Analysis for Point Processes,” *Journal of the American Statistical Association*, vol. 83, no. 401, pp. 9-27, 1988.
- [15] J. Zhuang, “Long-term earthquake forecasts based on the epidemic-type aftershock sequence (ETAS) model for short-term clustering,” *Research in Geophysics*, vol. 2:e8, pp. 52-57, 2012.
- [16] J. Woessner, A. Christophersen, J. Zechar and D. Monelli, “Building self-consistent, short-term earthquake probability (STEP) models: improved strategies and calibration procedures,” *Annals of Geophysics*, vol. 53, no. 3, pp. 141-154, 2010.
- [17] A. Schaefer, J. Daniell and F. Wenzel, “The SMART CLUSTER METHOD: Adaptive Earthquake Cluster Identification and Analysis in strong-seismic regions,” *in press*, 2016.
- [18] M. Båth, “Lateral inhomogeneities of the upper mantle,” *Tectonophysics*, vol. 2, no. 6, pp. 483-514, 1965.
- [19] L. Lawler and S. Rinnooy Kan, *The Traveling Salesman Problem. A Guided Tour of Combinatorial Optimization*, Chichester, 1985.
- [20] A. Frankel, “Mapping seismic hazard in central and eastern United States,” *Seismol. Res. Lett.*, vol. 66, pp. 8-21, 1995.
- [21] M. J. Werner, A. Helmstetter, D. D. Jackson and Y. Y. Kagan, “High-resolution long-term and short-term earthquake forecasts for California,” *Bulletin of the Seismological Society of America*, vol. 101, no. 4, pp. 1630-1648, 2011.
- [22] J. Zechar, “Evaluating earthquake predictions and earthquake forecasts: a guide for students and new researchers,” Community Online Resource for Statistical , <http://www.corssa.org>, 2010.
- [23] N. Ambraseys and C. Melville, *A history of Persian earthquakes*, Cambridge: Cambridge University Press, 1982.
- [24] I. Iervolino, M. Giorgio and E. Chioccarelli, “Closed-form aftershock reliability of damage-cumulating elastic perfectly-plastic systems,” *Earthquake Engineering & Structural Dynamics*, vol. 43, no. 4, pp. 613-625, 2014.
- [25] N. Luco, P. Bazzurro and C. Cornell, “Dynamic versus static computation of the residual capacity of a mainshock damaged building to withstand an aftershock,” in *13th World conference on earthquake engineering*, Vancouver, 2004.
- [26] M. Gerstenberger, S. Uma, N. Luco and H. Ryu, “Damage state exceedance probabilities from aftershocks,” GNS Science Consultancy Report, Retrieved from http://www.eqc.govt.nz/sites/public_files/1395-Damage-state-

exceedance-probabilities-aftershock.pdf, 2013/161.

- [27] K. Goda and M. Salami, "Inelastic seismic demand estimation of wood-frame houses subjected to mainshock-aftershock sequences," *Bulletin of Earthquake Engineering*, vol. 12, no. 2, pp. 855-874, 2014.
- [28] J. Daniell, B. Khazai, F. Wenzel and A. Vervaeck, "The CATDAT damaging earthquakes database," *Natural Hazards and Earth System Science*, vol. 11, no. 18, pp. 2235-2251, 2011.
- [29] A. King, D. Middleton, C. Brown, D. Johnston and S. Johal, "Insurance: Its role in recovery from the 2010-2011 Canterbury earthquake sequence," *Earthquake Spectra*, vol. 30, no. 1, pp. 475-491, 2014.
- [30] R. Cole, "Canterbury earthquakes 2010-2012: Insurance supervision in the first 2 years," in *NZSA Conference*, 2012.
- [31] "MORRISON and CROSS v VERO INSURANCE NEW ZEALAND LIMITED," 2014.
- [32] "RIDGECREST NZ LIMITED v IAG NEW ZEALAND LIMITED," 2014.
- [33] NCEDC, "Northern California earthquake data center," <http://www.quake.geo.berkeley.edu/anss/catalog-search.html>, 2016.
- [34] INGV, "Italian Seismic Bulletin," <http://iside.rm.ingv.it/iside/standard/index.jsp>.
- [35] NOAIG, "Seismic Catalogue," <http://www.gein.noa.gr/en/seismicity/earthquake-catalogs>, 2016.
- [36] W. Bakun, A. Johnston and M. Hopper, "Estimating locations and magnitudes of earthquakes in Eastern North America from Modified Mercalli Intensities," *Bulletin of the Seismological Society of America*, vol. 93, pp. 190-202, 2003.
- [37] T. Allen, D. Wald and C. Worden, "Intensity attenuation for active crustal regions," *Journal of Seismology*, vol. 16, pp. 409-433, 2012.
- [38] G. Ghosh and A. Mahajan, "Interpretation of Intensity Attenuation Relation of 1905 Kangra Earthquake with Epicentral Distance and Magnitude in the Northwest Himalaya Region," *Journal of the Geological Society of India*, vol. 77, 2011.
- [39] B. Papazachos, A. Kiratzi and B. Karacostas, "Towards a homogeneous moment-magnitude determination for earthquakes in Greece and the surrounding area," *Bulletin of the Seismological Society of America*, vol. 87, pp. 474-483, 1997.
- [40] M. Sørensen, D. Stromeyer and G. Grünthal, "Attenuation of macroseismic intensity. A new relation for the Marmara Sea region, Northwest Turkey," *Bulletin of the Seismological Society of America*, vol. 99, no. 2A, pp. 538-553, 2009.
- [41] D. Schorlemmer, M. Gerstenberg, S. Wiemer and D. Jackson, "Earthquake likelihood model testing," *Seismological Research Letters*, vol. 78, no. 17-29, p. 2007, 2007.